Available online at www.sciencedirect.com
ScienceDirect
Journal of Hazardous Materials 143 (2007) 448–454
Journal of Hazardous Materials
www.elsevier.com/locate/jhazmat

Effect of CeO_2 doping on catalytic activity of Fe_2O_3/γ-Al_2O_3 catalyst for catalytic wet peroxide oxidation of azo dyes

Yan Liu, Dezhi Sun *

School of Municipal & Environmental Engineering, Harbin Institute of Technology, Harbin 150090, China

Received 22 April 2006; received in revised form 12 September 2006; accepted 18 September 2006
Available online 20 September 2006

Abstract

In order to find a catalyst with high activity and stability for catalytic wet peroxide oxidation (CWPO) process under normal condition, with Fe_2O_3/γ-Al_2O_3 and Fe_2O_3–CeO_2/γ-Al_2O_3 catalysts prepared by impregnation method, the effect of CeO_2 doping on the structure and catalytic activity of Fe_2O_3/γ-Al_2O_3 for catalytic wet peroxide oxidation of azo dyes at 25 °C and atmospheric pressure is evaluated using BET, SEM, XRF, XRD, XPS and chemical analysis techniques, and test results show that, better dispersion and smaller size of Fe_2O_3 crystal can be achieved by adding CeO_2, and the content of chemisorbed oxygen can also be increased on the surface of catalyst. CWPO experimental results indicate that azo dyes in simulated wastewater can be efficiently mineralized and the catalytic activity of Fe_2O_3–CeO_2/γ-Al_2O_3 can be increased by about 10% compared with that of Fe_2O_3/γ-Al_2O_3 because of the promotion of the structural and redox properties of the ferric oxide by ceria doped. Leaching tests indicate that Fe_2O_3/γ-Al_2O_3 and Fe_2O_3–CeO_2/γ-Al_2O_3 are stable with a negligible amount of irons found in the aqueous solution after reaction for 2 h. It can therefore be concluded from results and discussion that in comparison with Fe_2O_3/γ-Al_2O_3, Fe_2O_3–CeO_2/γ-Al_2O_3 is a suitable catalyst, which can effectively degrade contaminants at normal temperature and atmospheric pressure.

Keywords: Catalytic wet peroxide oxidation; Promoted ceria catalyst; Azo dye; Wastewater treatment; Room temperature and atmospheric pressure

1. Introduction

The effluents from textile dyeing industry contain many organic pollutants and cause serious environmental problems for their color, high chemical oxygen demand (COD) and non-biodegradability [1,2], and catalytic wet oxidation (CWO) has been considered a very promising treatment method to destroy these organic pollutions in wastewater [3–5]. Because it is necessary to use more active oxidation agents to oxide wastewater at lower reaction temperature and pressure, a catalytic wet peroxide oxidation (CWPO) process has been developed in recent years [6]. By adding catalyst and oxidant, CWPO process can work well under mild condition without too much energy consumption, because the $^{\bullet}OH$ radicals generated in the reaction are highly oxidative, non-selective, and able to decompose many organic compounds including dyes and pesticides. Chen et al. [7] found that catalytic wet peroxide oxidation of reactive dyes can be successfully carried out with Cu-based catalysts, and more than 80% of TOC is removed from the solution in less than 15 min at 150 °C. Kim et al. [8] reported that complete removal of reactive dyes can be achieved within 20 min at 80 °C and normal atmospheric pressure by CWPO on Al-Cu pillared clay catalysts with bubbled air. Neamtu et al. [9] evaluated the degradation of a reactive azo dye, *Procion Marine H-EXL*, by CWPO process with Fe-exchanged Y zeolite as catalyst, and found more than 96% removal of color of 100 mg/L dye could be removed in 30 min at pH 5, $T = 50$ °C, 20 mmol/L H_2O_2 and 1 g/L $FeY_{11.5}$ which is equivalent to about 76% reduction of initial COD and 37% removal of initial TOC, but the degradation of organic pollutants with high concentration by CWPO at normal temperature and atmospheric pressure is not satisfactory.

Many investigators have been trying to improve the catalytic activity and stability of heterogeneous oxidation catalysts to enhance the efficiency of CWO [10–12], and cerium oxide and CeO_2-containing materials have been studied as catalysts, structural and electronic promoters used for heterogeneous catalysis over past years. It has been shown that cerium oxide promotes oxygen storage and release to enhance oxygen mobility, and

* Corresponding author. Tel.: +86 451 86283066; fax: +86 451 86283118.
E-mail address: sdzlab@126.com (D. Sun).

0304-3894/$ – see front matter © 2006 Elsevier B.V. All rights reserved.
doi:10.1016/j.jhazmat.2006.09.043

forms surface and bulk vacancies to improve the catalyst redox properties of the composite oxide when it is associated with transitional metal oxides [13–15].

In this paper, Fe_2O_3/γ-Al_2O_3 and Fe_2O_3–CeO_2/γ-Al_2O_3 catalysts are prepared by impregnation and characterized by BET nitrogen adsorption method, scanning electron microscope (SEM), X-ray fluorescence (XRF), X-ray diffraction (XRD), and X-ray photoelectron spectroscopy (XPS) techniques, and their catalytic activities were investigated by CWPO process at normal temperature and atmospheric pressure, so that the catalytic activity is correlated with catalyst characteristics and the effect of ceria on the properties of Fe_2O_3/γ-Al_2O_3 can be further understood. Three azo dyes, acid orange 52 (AO52), acid orange 7 (AO7) and reactive black 5 (RB5), were selected as model pollutants.

2. Experimental

2.1. Materials

All of reagents used for these experiments were analytical grade and were used as supplied. Deionized water was used in all experiments. The chemical structures of the three azo dyes are as shown in Fig. 1.

2.2. Catalysts preparation

The catalysts were prepared by impregnation method, and $Fe(NO_3)_3{\cdot}9H_2O$ and $Ce(NO_3)_3{\cdot}6H_2O$ were used as precursors, γ-Al_2O_3 (φ = 2–3 mm) as carrier. The Fe_2O_3/γ-Al_2O_3 was prepared by impregnation of 20 g γ-Al_2O_3 with 100 mL aqueous solution containing 0.1 mol/L $Fe(NO_3)_3$ for 12 h under room condition, then the samples were dried at 80 °C for 10 h and then dried at 110 °C for 2 h. The dried samples were calcined at 350 °C in an oven for 3h to obtain Fe_2O_3/γ-Al_2O_3 catalyst. The Fe_2O_3–CeO_2/γ-Al_2O_3, was prepared by consecutive impregnation in such a sequence that Ce was first loaded on γ-Al_2O_3 carrier by dipping of 20 g γ-Al_2O_3 in 100 mL aqueous solution containing 0.5 wt.% Ce (the weight ratio of Ce to carrier) for 12 h under room condition, and the samples were dried at 80 °C for 10 h and then dried at 110 °C for 2 h. The dried samples were calcined at 400 °C in an oven for 2 h, so that the intermediate CeO_2/γ-Al_2O_3 was obtained, and Fe was then loaded on CeO_2/γ-Al_2O_3 by impregnation, too, and following the same calcination procedure for the preparation of Fe_2O_3/γ-Al_2O_3 catalyst.

2.3. Characterization

The surface area, total pore volume and average pore size of samples were analyzed using the BET nitrogen adsorption method in an automated volumetric adsorption analyzer (model Quantachrome Autosorb-1).

The surface morphology of the samples was investigated using a Hitachi S-4700 SEM analyzer.

The elementary compositions of samples were determined using a AXIOS pw4400 XRF analyzer operating at 4 kW with Rh Kα used as X-ray source.

XRD analysis was carried out using a Rigaku D/max-rB X-ray diffractometer with a scanning range of 10–80° and a nickel-filtered Cu Kα radiation source at 45 kV and 45 mA, and a scanning speed of 5°/min.

XPS spectra were recorded using a PHI5700 analyzer with Al Kα ($h\nu$ = 1486.60 eV) used as X-ray source operating at 250 W and 12.5 kV. Kinetic energies of photoelectrons were measured using a hemispherical electrostatic analyzer working in the constant pass energy mode. The C 1s peak from the adventitious carbon-based contaminant, with the bind energy of 284.62 eV, is used as the reference for calibration. Curve fitting was carried out using a Physical Electronics PC-ACCESS ESCA-V6.0E program with a Gaussian–Lorentzian sum function. The Gaussian–Lorentzian mixing ratio was kept in the range 0.8–1.0.

2.4. Reaction procedures and analysis

CWPO process was carried out in a cylindrical reactor of 200 mL with a constant temperature waterbath. The reaction

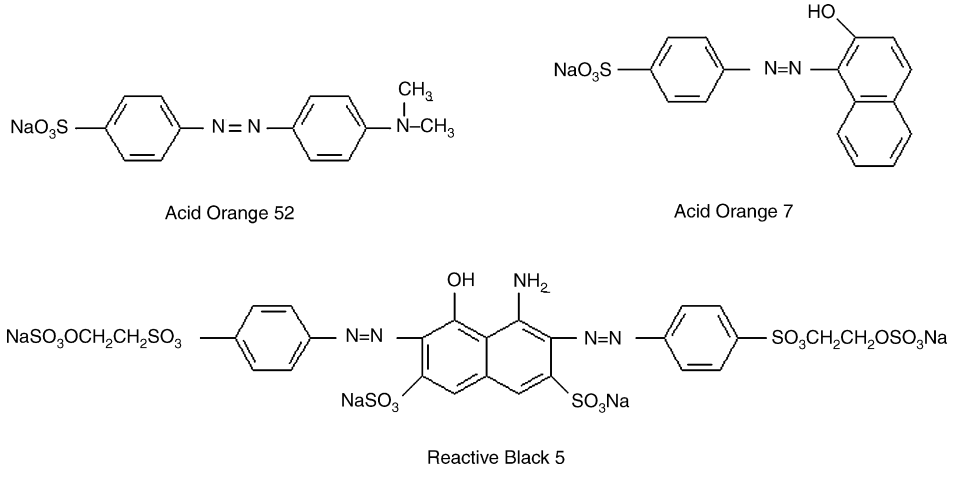

Fig. 1. Chemical structures of acid orange 52, acid orange 7 and reactive black 5.

Table 1
Results of BET tests

	BET surface area (m^2/g)	Total pore volume (mL/g)	Average pore size (nm)
γ-Al_2O_3	200.8	0.52	10.40
Fe_2O_3/γ-Al_2O_3	193.0	0.49	10.22
Fe_2O_3–CeO_2/γ-Al_2O_3	193.6	0.50	10.29

was conducted at atmospheric pressure and 25 °C. Three grams of catalysts and 33 mg H_2O_2 were introduced into 100 mL of aqueous dye wastewater with a dye concentration of 500 mg/L.

Liquid samples were taken out immediately at regular intervals for analysis of absorbance and total organic carbon (TOC). The visible light absorbance at the characteristic wavelength of the three dyes, 465 nm for AO52, 485 nm for AO7 and 600 nm for RB5, were measured using a UV-2550 Shimadzu UV-VIS spectrophotometer. TOC measurement was carried out with a TOC-V_{CPN} Shimadzu TOC analyzer. For evaluating the catalytic activity of catalysts, both color removal efficiency and TOC removal efficiency were calculated as shown below:

$$X\,(\%) = \frac{C_0 - C_t}{C_0} \times 100 \quad (1)$$

where C_0 and C_t are the initial and final absorbance values of dye, or the initial and final TOC, respectively.

An induced coupled plasma (ICP Model: Perkin-Elmer 5300DV) was used for determination of dissolved iron in solution and the samples were tested in duplicate.

3. Results and discussion

3.1. BET, SEM and XRF analysis of catalysts

The BET surface area, total pore volume and average pore size of the investigated catalysts are listed in Table 1. Fe_2O_3/γ-Al_2O_3 catalyst and Fe_2O_3–CeO_2/γ-Al_2O_3 catalyst reduced the surface area from 200.8 to 193.0 m^2/g and 193.6 m^2/g, respectively, and due to the introduction of Fe and Ce, the total pore volume and average pore size of the catalysts also reduced compared with the carrier. The effect of CeO_2 doping on the pore structure of Fe_2O_3/γ-Al_2O_3 catalyst is not obvious.

The dispersion of Fe_2O_3 particles on the surface of Fe_2O_3/γ-Al_2O_3 and Fe_2O_3–CeO_2/γ-Al_2O_3 catalysts is as shown in Fig. 2. It can be seen that from Fig. 2(a) slight aggregates of Fe_2O_3 particles are observed on the surface of Fe_2O_3/γ-Al_2O_3 catalyst, but the better dispersion can be achieved by doping of CeO_2 as shown in Fig. 2(b), and a smaller crystal size can also be seen from Fig. 2(b) compared with Fig. 2(a).

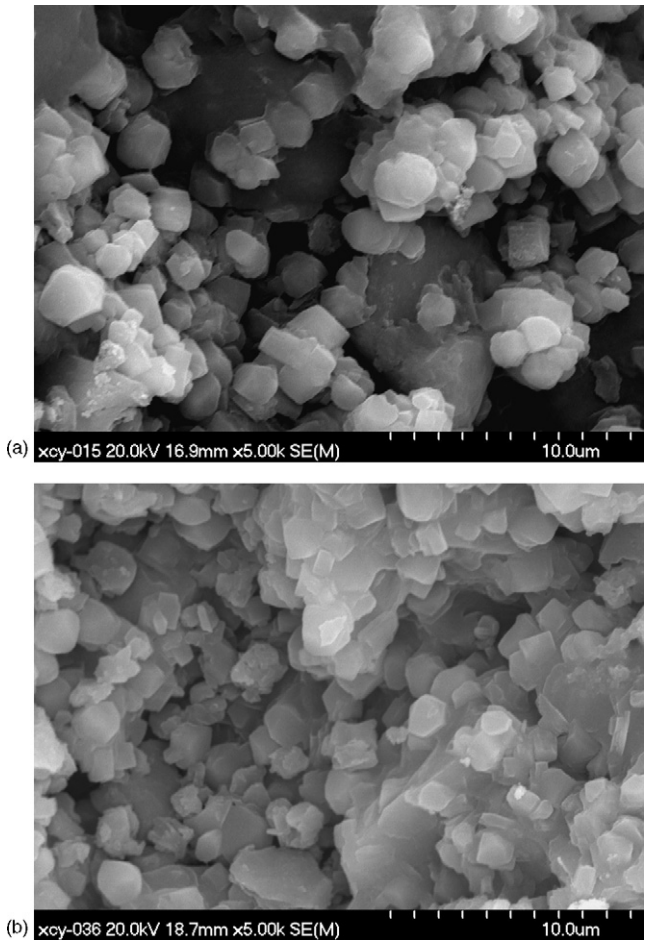

Fig. 2. SEM image of catalysts: (a) Fe_2O_3/γ-Al_2O_3; (b) Fe_2O_3–CeO_2/γ-Al_2O_3.

The component contents of the two investigated catalysts analyzed by XRF are shown in Table 2. The content of Fe in Fe_2O_3/γ-Al_2O_3 catalyst increases from 1.907% to 2.207% by introduction of Ce, although the content of Ce is only 0.390% in Fe_2O_3–CeO_2/γ-Al_2O_3 catalyst. This shows that ceria can promote the structure of supports, so that the loading of Fe in the catalyst is improved.

3.2. XRD analysis of catalyst

Fig. 3 shows the XRD patterns of γ-Al_2O_3 carrier, Fe_2O_3/γ-Al_2O_3 catalyst and Fe_2O_3–CeO_2/γ-Al_2O_3 catalyst. γ-Al_2O_3 phase can easily be seen in its pattern. The peaks characterizing α-Fe_2O_3 crystal can be seen in the pattern of Fe_2O_3/γ-Al_2O_3 catalyst, but become weaker or fade away in the pattern of Fe_2O_3–CeO_2/γ-Al_2O_3 catalyst, which verifies the addition of CeO_2 promotes the dispersion of Fe_2O_3 particles and get the crystal size of Fe_2O_3 smaller. The peaks charac-

Table 2
Results of XRF analysis

Catalysts	Al (%)	O (%)	Fe (%)	Ce (%)	Na (%)	Si (%)
Fe_2O_3/γ-Al_2O_3	48.341	49.641	1.907	0	0.063	0.048
Fe_2O_3–CeO_2/γ-Al_2O_3	47.835	49.679	2.207	0.390	0.031	0.038

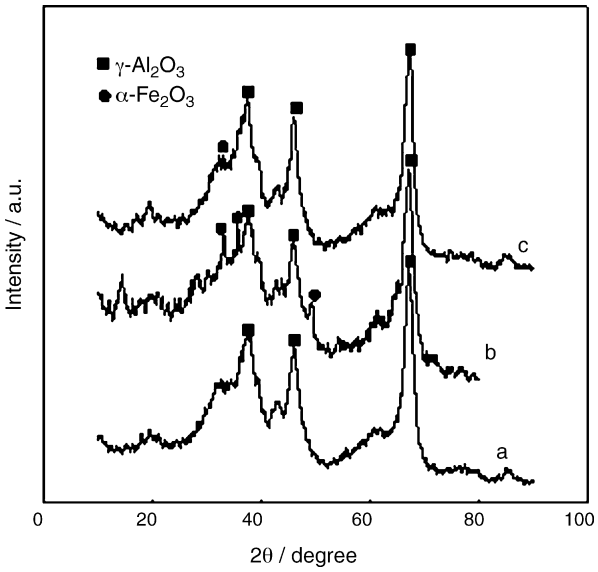

Fig. 3. XRD patterns of catalysts: (a) γ-Al_2O_3; (b) Fe_2O_3/γ-Al_2O_3; (c) Fe_2O_3–CeO_2/γ-Al_2O_3.

terizing CeO_2 crystals cannot be seen in the XRD pattern of Fe_2O_3–CeO_2/γ-Al_2O_3 catalyst, because the content of Ce doped in Fe_2O_3–CeO_2/γ-Al_2O_3 catalyst is too low.

3.3. XPS analysis of catalysts

It can be seen from Fig. 4 that the Fe 2p3/2 peak of Fe_2O_3/γ-Al_2O_3 catalyst appears at 710.9 eV, while that of Fe_2O_3–CeO_2/γ-Al_2O_3 catalyst appears at 710.8 eV, which is ascribable to Fe_2O_3 [16,17]. There is no great change in Fe 2p3/2 peak before and after CeO_2 doping, and this indicates that CeO_2 has only a slight effect on the chemical state of Fe_2O_3.

The characteristic peaks of Ce cannot be observed in the survey XPS pattern of Fe_2O_3–CeO_2/γ-Al_2O_3 catalyst possibly because the loaded content of Ce is too low to be detected,

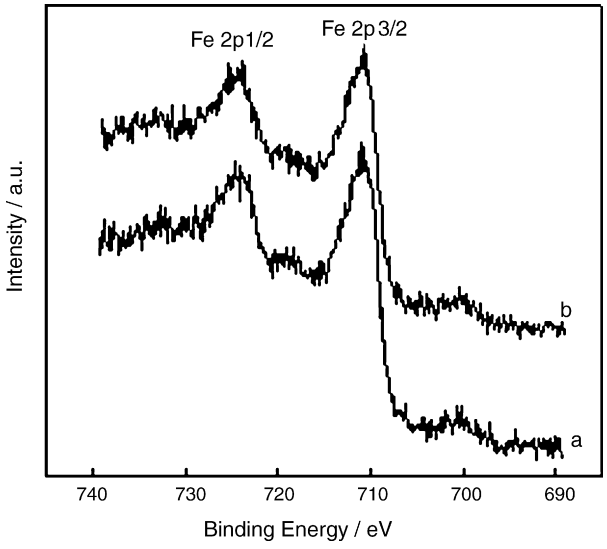

Fig. 4. Fe 2p XPS patterns of catalysts: (a) Fe_2O_3/γ-Al_2O_3; (b) Fe_2O_3–CeO_2/γ-Al_2O_3.

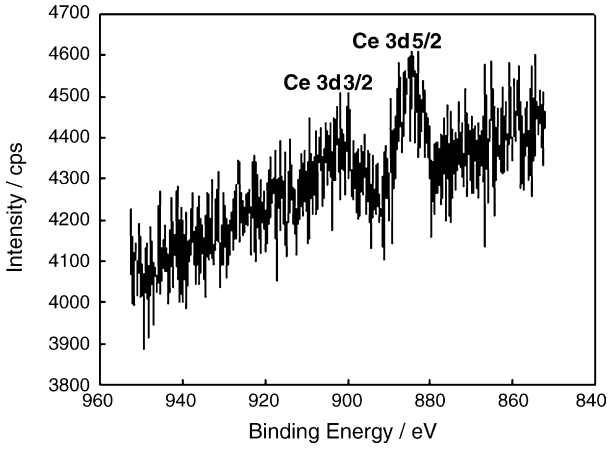

Fig. 5. Ce 3d XPS spectra of CeO_2/γ-Al_2O_3.

and Fe_2O_3–CeO_2/γ-Al_2O_3 catalyst is prepared by successive impregnation and Ce is covered by Fe_2O_3. It is well known that XPS can be used to analyze the surface and a limited (5–10 nm) depth of catalysts only, and so Ce cannot be detected on the surface of Fe_2O_3–CeO_2/γ-Al_2O_3 catalyst.

In order to investigate the existence of Ce in Fe_2O_3–CeO_2/γ-Al_2O_3 catalyst, XPS is employed to analyze the surface of intermediate CeO_2/γ-Al_2O_3. Fig. 5 shows Ce 3d XPS pattern of CeO_2/γ-Al_2O_3, and Ce 3d5/2 peak can be observed at the binding energy of 882.4 eV, which is ascribable to CeO_2 [18].

It can be seen from Fig. 6 that the O 1s XPS peaks are asymmetric, which indicates that different types of oxygen exist on the catalyst surface. The addition of CeO_2 increases the binding energy of O 1s peak from 529.9 to 530.9 eV, and this shows the existence of oxygen on the surface had been affected by CeO_2.

In order to investigate the further details of oxygen on the surface, O 1s spectra are fitted roughly as shown in Fig. 7. The O 1s peaks can be fitted into three peaks: One peak with the highest binding energy can be attributed to the chemisorbed oxygen on the surface of catalysts; one moderate is due to the lattice oxygen of Al_2O_3, and the last peak is assigned to the lattice oxygen of

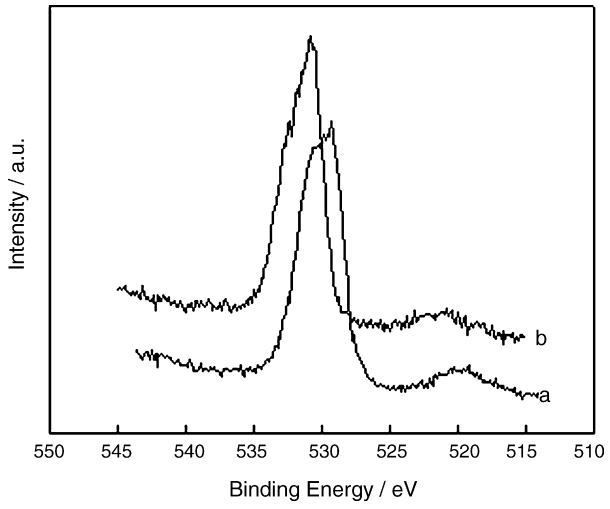

Fig. 6. O 1s XPS patterns of catalysts: (a) Fe_2O_3/γ-Al_2O_3; (b) Fe_2O_3–CeO_2/γ-Al_2O_3.

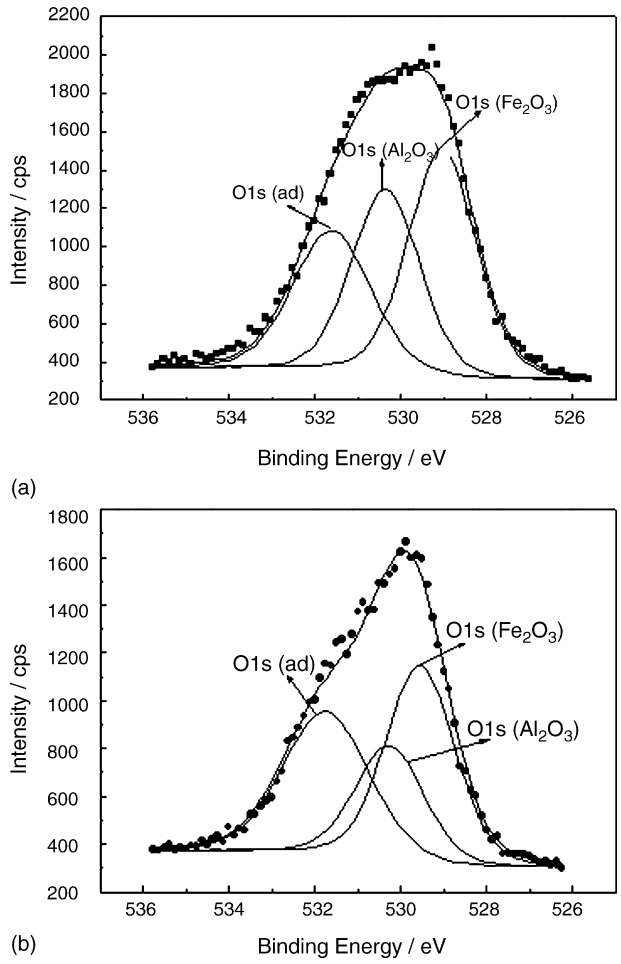

Fig. 7. O 1s curves fitting of catalysts: (a) Fe_2O_3/γ-Al_2O_3; (b) Fe_2O_3–CeO_2/γ-Al_2O_3.

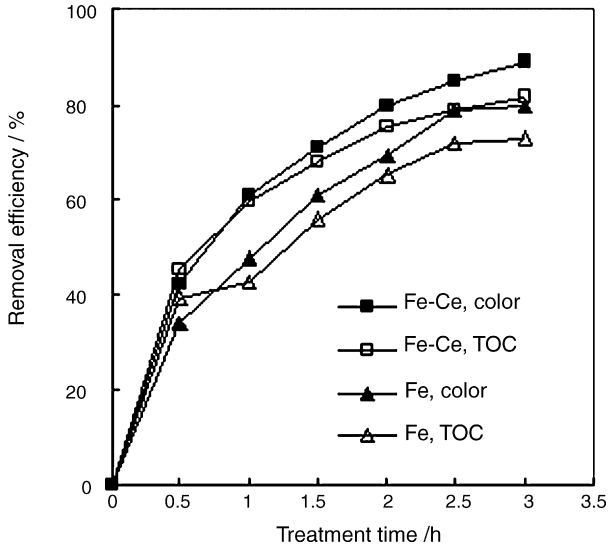

Fig. 8. Degradation efficiency of AO52 in CWPO with Fe_2O_3/γ-Al_2O_3 and Fe_2O_3–CeO_2/γ-Al_2O_3 as catalyst.

Fe_2O_3 [16], i.e., there exist two types of oxygen on the surface of catalysts, one is the characteristic lattice oxygen with low binding energy, and the other is most likely to be chemisorbed oxygen with high binding energy. According to the studies [13,19], the chemisorbed oxygen, which has higher mobility than lattice oxygen, can take an active part in the oxidation process and greatly improve the catalyst activity. In the CWPO process, $^{\bullet}OH$ can be generated not only by reacting ferrous salts with H_2O_2 [20], but also by a free radical chain auto-oxidation process, which can be described as follows [21]:

$$RH + Fe^{3+} \rightarrow R^{\bullet} + H^{+} + Fe^{2+} \text{ (initiation)} \quad (2)$$

$$R^{\bullet} + O_2 \rightarrow RO_2^{\bullet} \text{ (propagation)} \quad (3)$$

$$RO_2^{\bullet} + RH \rightarrow ROOH + R^{\bullet} \text{ (propagation)} \quad (4)$$

$$ROOH \rightarrow RO^{\bullet} + {}^{\bullet}OH \text{ (autocatalytic decomposition)} \quad (5)$$

Reaction (2) occurs on the catalyst surface and is a fast reaction, and reactions (3) and (4) are the key steps to produce $^{\bullet}OH$, and so, increasing the chemisorbed oxygen content on the surface of the catalysts expedites reactions (3) and (4) to produce $^{\bullet}OH$, thereby promoting the activity of the catalysts.

It can be seen from Table 3 that the addition of CeO_2 increases the percentage of the chemisorbed oxygen in the total oxygen, in other words, CeO_2 doped improves the catalytic activity of Fe_2O_3/γ-Al_2O_3.

3.4. Analysis of catalytic activity

Figs. 8–10 summarize the time dependence of color removal efficiencies and TOC removal efficiencies of three dyes in the CWPO process with Fe_2O_3/γ-Al_2O_3 and Fe_2O_3–CeO_2/γ-Al_2O_3 used as catalysts, respectively. It can be seen that two catalysts show promising catalytic activity during the catalytic wet oxidation of three azo dyes at 25 °C and atmospheric pressure with high mineralization efficiency achieved in this process. After being used to treat the simulated wastewater containing 500 mg/L of AO52, the removal efficiency of color and TOC of Fe_2O_3–CeO_2/γ-Al_2O_3 catalyst in 3 h are 88.77% and 81.44%, respectively, and the other two dyes, AO7 and RB5, can also be degraded efficiently.

Table 3
XPS data of O element on the surface of the two catalysts

Catalysts	Binding energy (eV)			Percentage of O_{ad} or O_L to O_T (%)		
	O_{ad}	O_L (Al_2O_3)	O_L (Fe_2O_3)	O_{ad}	O_L (Al_2O_3)	O_L (Fe_2O_3)
Fe_2O_3/γ-Al_2O_3	531.61	530.36	529.64	28.10	31.86	40.05
Fe_2O_3–CeO_2/γ-Al_2O_3	531.75	530.26	529.55	36.22	23.39	40.39

O_{ad}: the chemisorbed oxygen; O_L: the latter oxygen; O_T: the total oxygen.

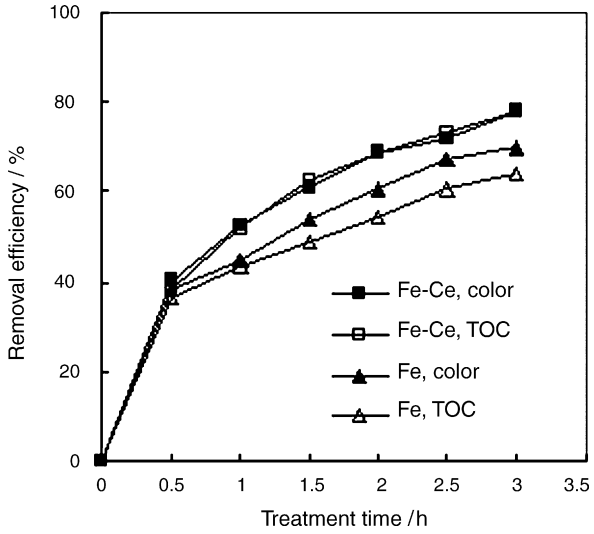

Fig. 9. Degradation efficiency of AO7 in CWPO with Fe_2O_3/γ-Al_2O_3 and Fe_2O_3–CeO_2/γ-Al_2O_3 as catalyst.

It can be concluded from the results of CWPO that the degradation efficiency can be improved by about 10% by using ceria promoted Fe_2O_3/γ-Al_2O_3 catalyst under the same reaction condition. The promoted catalytic activity can be attributed to the special ability of Ceria for two reasons: (1) better dispersion and smaller size of Fe_2O_3 crystal achieved when CeO_2 doped increases the number of effectively active sites, and this increase helps the instant production of more $^{\bullet}OH$, and CeO_2 can act as a structural promoter of Fe_2O_3/γ-Al_2O_3 catalyst; (2) the addition of CeO_2 increases the content of chemisorbed oxygen on the surface of Fe_2O_3/γ-Al_2O_3 catalyst, thereby improving the redox properties of composite catalysts, and so, CeO_2 can act as an electronic promoter of Fe_2O_3/γ-Al_2O_3 catalyst. Therefore, the catalytic activity of Fe_2O_3–CeO_2/γ-Al_2O_3 catalyst is higher than that of Fe_2O_3/γ-Al_2O_3 catalyst in CWPO process under normal condition.

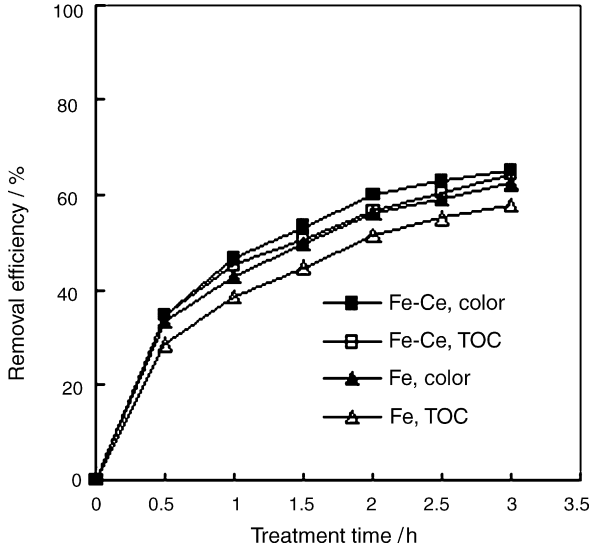

Fig. 10. Degradation efficiency of RB5 in CWPO with Fe_2O_3/γ-Al_2O_3 and Fe_2O_3–CeO_2/γ-Al_2O_3 as catalyst.

The treatment efficiency of Fe_2O_3/γ-Al_2O_3 or Fe_2O_3–CeO_2/γ-Al_2O_3 without H_2O_2 is also investigated, and only about 30% decolorization efficiency was achieved in 3 h with AO52 as model pollution, which verifies the main reason for degradation of dyes is catalytic oxidation, not adsorption. In addition, the data presented in Figs. 8–10 indicates that methyl orange is easier to be degraded than acid orange 7, and reactive black 5 is the most difficult one to be degraded. The relative order for degradation efficiency is directly proportional to the molecular weight and structural complexity of dye.

The tests conducted to assess the catalytic activity of same batch of Fe_2O_3/γ-Al_2O_3 and Fe_2O_3–CeO_2/γ-Al_2O_3 used in consecutive oxidation runs with the same catalysts load under the same reaction conditions show that the catalytic activity decreases fast in the successive runs, and the decolorization efficiency of 500 mg/L of methyl orange in 3h decreases from 88.77% for the first run to 53.66% for the third run by using Fe_2O_3–CeO_2/γ-Al_2O_3 as catalyst, and from 79.67% for the first run to 50.63% for the third run by using Fe_2O_3/γ-Al_2O_3 as catalyst, which indicates that the doping of Ce does not improve the service life of Fe_2O_3/γ-Al_2O_3. Much effort should be given to the improvement of catalyst service life in the next study.

3.5. Leaching tests

During the CWPO process, the components may be leached out from the catalysts. To investigate the stability of Fe_2O_3/γ-Al_2O_3 and Fe_2O_3–CeO_2/γ-Al_2O_3 with respect to metal leaching, the concentrations of dissolved Fe, Al and Ce in the solution after catalytic oxidation for 2 h are analyzed using ICP, and the concentrations of three metallic ions are 0.04, 0.36 and 0 mg/L, respectively while Fe_2O_3/γ-Al_2O_3 is used as catalyst, and 0.01, 0.39 and 2.16 mg/L, respectively while Fe_2O_3–CeO_2/γ-Al_2O_3 is used as catalyst. Under the reaction conditions employed for this research, the two catalysts under study show an excellent chemical stability with negligible leaching ions, and the doping of Ce has no obvious effect on the stability of the catalyst.

4. Conclusions

Three azo dyes can be efficiently degraded with Fe_2O_3/γ-Al_2O_3 and Fe_2O_3–CeO_2/γ-Al_2O_3 used as catalysts in a CWPO process under standard atmospheric conditions. Fe_2O_3–CeO_2/γ-Al_2O_3 has shown more promising catalytic activity compared with Fe_2O_3/γ-Al_2O_3. From the results of catalysts characterization and catalytic tests, it can be concluded that better dispersion and smaller size of Fe_2O_3 crystal can be achieved when CeO_2 is doped, which increases the number of effectively active sites. Moreover, the addition of CeO_2 increases the content of chemisorbed oxygen on the surface of Fe_2O_3/γ-Al_2O_3 catalyst, and improves the redox properties of composite catalysts. As a result, Fe_2O_3–CeO_2/γ-Al_2O_3 catalyst can improve the degradation efficiency by about 10% compared with Fe_2O_3/γ-Al_2O_3 catalyst under the same reaction conditions. Leaching tests showed that the doping of Ce has no obvious effect on the stability of catalyst and the two catalysts under study show an excellent stability with negligible leaching ions in the CWPO

process. It can therefore be concluded from Section 3 above that in comparison with Fe_2O_3/γ-Al_2O_3, Fe_2O_3–CeO_2/γ-Al_2O_3 is a suitable catalyst with high activity and stability for catalytic wet peroxide oxidation (CWPO) process under normal condition

CWPO process is a promising technology which can be used to treat aqueous solutions containing organics under standard atmospheric conditions with excellent performance, although much efforts has to be directed to the improvement of catalyst service life.

Acknowledgements

The authors would like to thank the financial support from the National Basis Research Program of China (973 Program, No. 2004CB418505) and the Foundation for Excellent Youth of Heilongjiang Province of China.

References

[1] U. Zissi, G. Lyberatos, Azo-dye biodegradation under anoxic conditions, Water Sci. Technol. 34 (1996) 495–500.
[2] K. Golka, S. Kopps, Z.W. Myslak, Carcinogenicity of azo colorants: influence of solubility and bioavailability, Toxicol. Lett. 151 (2004) 203–210.
[3] F. Luck, Wet air oxidation: past, present and future, Catal. Today 53 (1999) 81–91.
[4] Q. Wu, X. Hu, P.L. Yue, X.S. Zhao, G.Q. Lu, Copper/MCM-41 as catalyst for the wet oxidation of phenol, Appl. Catal. B: Environ. 32 (2001) 151–156.
[5] D.K. Lee, I.C. Cho, G.S. Lee, S.C. Kim, D.S. Kim, Y.K. Yang, Catalytic wet oxidation of reactive dyes wtih H_2/O_2 mixture on Pd-Pt/Al_2O_3 catalysts, Sep. Purif. Technol. 34 (2004) 43–50.
[6] G. Centi, S. Perathoner, T. Torre, M.G. Verduna, Catalytic wet oxidation with H_2O_2 of carboxylic acids on homogeneous and heterogeneous Fenton-type catalysts, Catal. Today 55 (2000) 61–69.
[7] G. Chen, L. Lei, P.L. Yue, Wet oxidation of high-concentration reactive dyes, Industr. Eng. Chem. Res. 38 (1999) 1837–1843.
[8] S.C. Kim, D.K. Lee, Preparation of Al–Cu pillared clay catalysts for the catalytic wet oxidation of reactive dyes, Catal. Today 97 (2004) 153–158.
[9] M. Neamţu, C. Zaharia, C. Catrinescu, A. Yediler, M. Macoveanu, A. Kettrup, Fe-exchanged Y zeolite as catalyst for wet peroxide oxidation of reactive azo dye *Procion Marine H-EXL*, Appl. Catal. B: Environ. 48 (2004) 287–294.
[10] Q. Zhang, K.T. Chuang, Kinetics of wet oxidation of black liquor over a Pt–Pd–Ce/alumina catalyst, Appl. Catal. B: Environ. 17 (1998) 321–332.
[11] A.M.T. Sliva, A.C.M. Oliveira, R.M. Quinta-Ferreira, Catalytic wet oxidation of ethylene glycol: kinetics of reaction on a Mn–Ce–O catalyst, Chem. Eng. Sci. 59 (2004) 5291–5299.
[12] I.P. Chen, S.S. Lin, C.H. Wang, L. Chang, J.-S. Chang, Preparing, characterizing an optimal supported ceria catalyst for the catalytic wet air oxidation of phenol, Appl. Catal. B: Environ. 50 (2004) 49–58.
[13] H. Chen, A. Saysri, A. Adnot, F. Larachi, Composition-activity effects of Mn–Ce–O composites on phenol catalytic wet oxidation, Appl. Catal. B: Environ. 32 (2001) 195–204.
[14] F. Larachi, J. Pierre, A. Adnot, A. Bernis, Ce 3d XPS study of composite $Ce_xMn_{1-x}O_{2-y}$ wet oxidation catalysts, Appl. Surf. Sci. 195 (2002) 236–250.
[15] G. Neri, A. Pistone, C. Milone, S. Galvagno, Wet air oxidation of *p*-coumaric acid over promoted ceria catalysts, Appl. Catal. B: Environ. 38 (2002) 321–329.
[16] C.D. Wagner, W.M. Riggs, L.E. Davis, J.F. Moulder, G.E. Muilenberg, Handbook of X-Ray Photoelectron Spectroscopy, 55344, Perkin-Elmer Corporation, Physical Electronics Division, Eden Prairie, Minn, 1979.
[17] B.J. Tan, K.J. Klabunde, P.M.A. Sherwood, X-ray photoelectron-spectroscopy studied of solvated metal atom dispersed catalysts —monometallic iron and bimetallic iron cobalt particles on alumina, Chem. Mater. 2 (1990) 186–191.
[18] A. Dauscher, L. Hilaire, F. LeNormand, W. Muller, G. Maire, A. Vasquez, Characterization by XPS and XAS of supported Pt/TiO_2–CeO_2 catalysts, Surf. Interf. Anal. 16 (1990) 341–346.
[19] S.S. Lin, C.L. Chenb, D.J. Chang, C.C. Chen, Catalytic wet air oxidation of phenol by various CeO_2 catalysts, Water Res. 36 (2002) 3009–3014.
[20] C.L. Hsueh, Y.H. Huang, C.C. Wang, C.Y. Chen, Degradation of azo dyes using low iron concentration of Fenton and Fenton-like system, Chemosphere 58 (2005) 1409–1414.
[21] I. Arslan-Alaton, J.L. Ferry, Application of polyoxotungstates as environmental catalysts: wet air oxidation of acid dye Orange II, Dyes Pigm. 54 (2002) 25–36.